ACS Macro Letters

Letter

pubs.acs.org/macroletters

Length-Dependent Assembly of a Stiff Polymer Chain at the Interface of a Carbon Nanotube

Ruohai Guo,† Zhen Tan,† Kunlun Xu, and Li-Tang Yan*

Advanced Materials Laboratory, Department of Chemical Engineering, Tsinghua University, Beijing 100084, People's Republic of China

ABSTRACT: We perform computer simulations to explore the suprastructures and their formation mechanism in the length-dependent assembly of a stiff polymer chain on the carbon nanotube surface. Three types of local conformations, that is, helical wrapping along the nanotube threadline, nonhelical loop, and straight extension along the nanotube, are identified in the very stiff polymer, depending on its length. It is revealed that the high elastic energy penalty and the large length of a long stiff polymer hinder its conformation transition on the nanotube, which impairs the match between the polymer beads and the structural details of the underlying nanotube surface and thereby weakens the polymer-nanotube interaction. A preferred chain length with an energy minimum is documented for the first time in the self-assemble of a stiff polymer at the nanotube interface. These data significantly advance our understanding of the superstructure formation by self-assembly of various chain-like molecules (e.g., polymer, surfactants, DNA, peptides, etc.) on carbon nanotube.

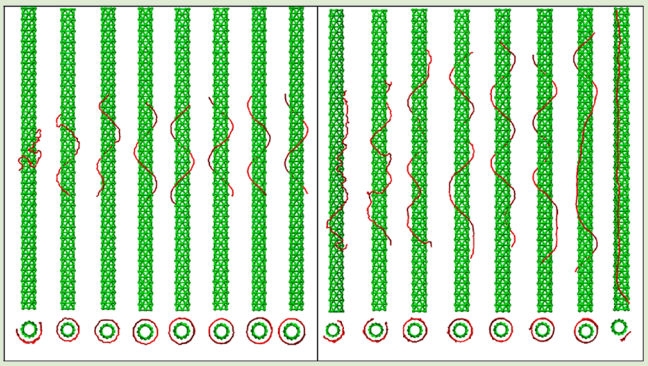

Noncovalent interactions with the surface of single-walled carbon nanotubes (SWNTs) enable purification, dispersion, and multifunctional applications while preserving the intrinsic properties of the SWNTs.[1,2] In particular, much research on noncovalent wrapping around the surface of SWNTs with chain-like polymers, including π-conjugated polymers,[3] carbohydrates,[4] peptides,[5] and DNAs,[6] has been reported. An essential ingredient in superstructure formation through the self-assembly of a polymer at SWNT interface is the chain stiffness of the underlying chain backbone controlled by the local chemical structures.[7−11] Efforts have been made to investigate the influence of the intrinsic stiffness of a polymer on its complex with a SWNT.[12−16] For instance, the simulation of polymer absorption on a smooth cylindrical surface indicated that the adsorbed conformations depend on chain stiffness: ranging from randomly adsorbed conformations of the flexible chain to perfect helical conformation of the semiflexible chains.[12]

One particular aspect of the problem that has not been studied and could be of great relevance concerns the role of the chain length of the stiff polymer. The physics of the chain length effect emerges upon considering the persistence length, that is, chains comprising single persistence length deform as bendable rods while chains comprising many persistent segments behave as a random walk opposed by loss of configuration entropy. This aspect is critically important when the structural details of both polymer and underlying nanotube surface are considered.[17−19] In fact, a recent work studying the filament bonding to a deformable cylindrical surface remainders that the structural details of the underlying surface cannot be neglected when the monomer size is comparable to the size of the surface beads.[19] However, most of prior research based on the smooth cylindrical surface cannot provide explicit insight into this effect. Actually, the stiff polymer interaction with cylinders of certain contacting regions is a generic physical problem. The nucleosome in chromatin, where the DNA of a stiff polymer chain is coiled in almost two turns of a left-handed helix around the histone octamer, is another dramatic example of it.[20−22]

Here, we show how the chain length of a stiff polymer influences its self-assembly at the nanotube interface and analyzes the physical reasons behind it. The chain length dependent conformations and interactions of the stiff polymer are considered through the elaborate examination of the structural details within the system. In addition, a preferred chain length with an energy minimum is found for the first time in the self-assembly of a stiff polymer at the nanotube interface. The findings and their physical mechanism demonstrated in the letter are quite general and are applicable to the generic physical problem of a stiff string interacting with the detailed structures of a cylindrical surface. Practically the chain-like polymers used in the present simulations more approximate to the conjugated linear polymers.

We use the dissipative particle dynamics (DPD) technique, which extends the simulation scales of time and space to be appropriate to the study of polymer−SWNT nanocomposites.

Received: May 7, 2012
Accepted: July 6, 2012
Published: July 17, 2012

An effective coarse-grained methodology of the SWNT is used in the modeling, where 24 carbon atoms in an armchair SWNT are lumped together into one DPD bead.[23] This methodology based on DPD method has proved its validity and efficiency in the simulations of the mechanical behaviors and structures of SWNTs.[23,24] The present simulations are carried out using four different interaction forces between beads, that is, the conservative interaction force F^C, dissipative force F^D, random force F^R, and spring force F^S. The interaction forces are treated as pairwise additive. The detailed forms of F^C, F^D, and F^R, which can be found elsewhere,[25] are of short-range with a fixed cutoff distance, r_c. The interaction parameters used here are similar with those used by Liba et al.[23] and in our previous work.[24] The finite polymer concentration effects will affect the assembled structures while the study focusing on the self-assembly of one polymer chain on the SWNT facilitates exploring the nature of the structural formation and interaction within the system. Thereby, to effectively clarify the polymer-SWNT interaction, only one polymer chain is included in each simulation system. The polymer chain consists of L beads in which the neighboring beads are connected by bonds. These bonds are represented by a harmonic spring potential $U_{bond} = K_b((r - b)/r_c)^2$, where $K_b = 64$ and $b = 0.5r_c$ (with $r_c \approx 1$ nm)[23] are the bond constant and the equilibrium bond length, respectively.[26] Additionally, we include a three-body stiffness potential along the polymer chain of the form $U_{angle} = (K_a/2)(\cos(\alpha) - \cos(\alpha_0))^2$.[27] Various values of K_a are chosen to mimic the change of the chain stiffness. Physically, K_a represents the chain stiffness of the underlying chain backbone controlled by the local chemical structures. For example, as to three polymer chains with similar structures, that is, polystyrene (PS), poly(phenylacetylene) (PPA), and poly(*p*-phenylenevinylene) (PPV), PS is rather flexible because its σ-bonds between repeating units allow easy rotation around the axis of the backbone, whereas PPA is semiflexible because of its completely conjugated backbone structure; PPV is a rigid linear molecular with a conjugated aromatic ring backbone structure.[13] The persistence length of the polymer chain (l_p) can be experimentally measured to quantify the stiffness of polymers with various chemical structures. In this letter, the relationship between K_a and l_p is thereby determined to indicate a detailed correlation between our simulations results and the possible experimental systems (see Figure 2B). An armchair (12, 12) SWNT with radius about 0.815 nm is used in the simulations. The polymer−SWNT interaction is represented by the Lennard-Jones (LJ) potential,[27,28] $U = 4\varepsilon(-(\sigma_{vdw}/r_{ij})^6 + (\sigma_{vdw}/r_{ij})^{12})$, where ε and σ_{vdw} are the well depth of the potential and the characteristic length at the equilibrium distance, and r_{ij} is the distance between beads i and j. In the present simulation, $\varepsilon = 5.57\ k_BT$ is used based on the calculation of the graphitic potential and σ_{vdw} is set to 0.445 nm so that the van der Waals (vdW) force does not cause bond crossing. The simulation box is $24r_c \times 24r_c \times 48r_c$ in size and with periodic boundary condition in all directions, which is large enough to avoid the finite size effects. The time step of $\Delta t = 0.005\tau$ is chosen ensuring the accurate temperature control over the simulation system.[29] The typical simulation run of 10^6 steps corresponds to a time of 0.39 μs, which ensures the conformation equilibrium of a polymer chain at the SWNT interface.

To probe the influence of chain length on the polymer conformation at the nanotube interface, a series of simulations are performed, where the polymer chain is placed in the vicinity of the SWNT surface within the cutoff distance of vdW interaction at the initial stage. The representative equilibrium conformations of a short ($L = 50b$) and a long ($L = 96b$) polymers with a systematic increase of chain stiffness are presented in Figure 1A,B. When the chain stiffness is not too high ($K_a \leq 300$), both the short and the long polymers prefer the perfect helical wrapping conformation around the nanotube with increasing K_a, reproducing the Monte Carlo simulation results with a smooth cylindrical surface.[12] In particular, the very flexible polymer chains at $K_a = 0$ present "cloud" conformation, allowing them to retain high entropy by sampling a large number of conformations. Increasing the chain stiffness from $K_a = 0$−300 allows for the formation of multiple helices resulting from further optimization of the absorbed conformations in order to maximize chain entropy and the polymer−nanotube interaction.[12] Figure 1A shows that the perfect helical conformation can be held for the short polymer with further increasing the chain stiffness. However, our simulations demonstrate that excessively increasing the stiffness of the long polymer can penalize its helical wrapping conformation (see the snapshots when $K_a > 300$ in Figure 1B), which has not been predicted by prior simulations but is in agreement with the experimental result considering the stiffness-dependent polymer wrapping onto SWNTs.[16] To gain insight into the conformational difference between the short and the long polymers at the large values of K_a, we calculate the averaged interaction energy between the beads of the polymer and the nanotube, U_a, which characterizes the attraction strength between the polymer chain and the SWNT. A lower U_a indicates a stronger polymer−SWNT attraction and vice versa. Figure 1C displays the equilibrated U_a as a function of K_a for the short and the long polymer chains. The dashed

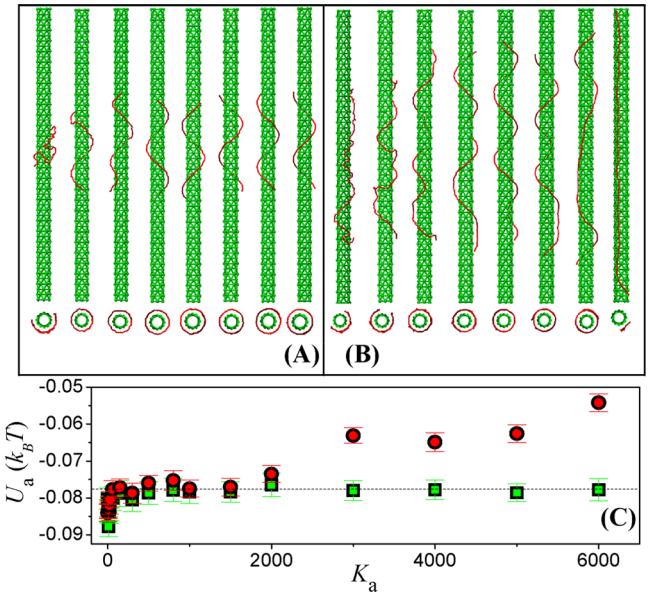

Figure 1. (A, B) Representative equilibrium conformations of a polymer absorbed at the SWNT interface. The contour lengths of the polymer chains in columns A and B are $L = 50b$ and $96b$, respectively. The top and bottom snapshots display the side and front views of the polymer conformation at a certain value of K_a. In columns (A) and (B), the values of K_a are 0, 20, 60, 300, 1000, 2000, 4000, and 6000 from left to right. (C) U_a as a function of K_a at various contour lengths of the polymer: (green) $L = 50b$ and (red) $L = 96b$. The dashed line is to guide the eye.

dx.doi.org/10.1021/mz300221s | *ACS Macro Lett.* 2012, 1, 977−981

line in this figure clarifies that, in response to the increase of chain stiffness from $K_a > 300$, the polymer−nanotube attraction is almost invariant for the short polymer, while it is obviously weakened for the long one, corresponding to the polymer conformations demonstrated in Figure 1A,B. Clearly, the chain length plays a significant role in the conformation and interaction of a stiff polymer in the polymer−nanotube complex, although this effect is considerably slight for the flexible polymer.

To access the physical mechanism of the chain length dependent conformation and interaction of the stiff polymer, in Figure 2A we present the averaged polymer−nanotube

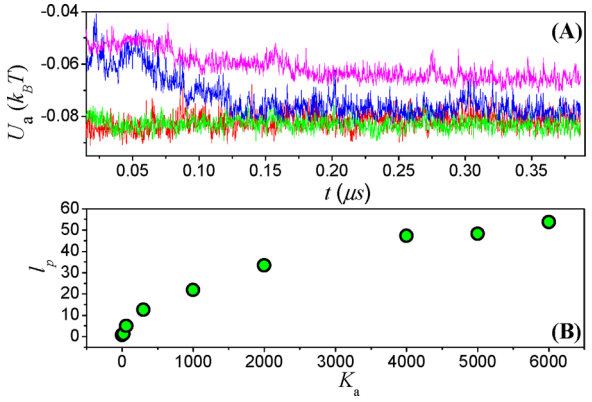

Figure 2. (A) Time evolution of U_a at different values of L and K_a: (red) $L = 50b$ and $K_a = 0$, (green) $L = 96b$ and $K_a = 0$, (blue) $L = 50b$ and $K_a = 4000$, and (pink) $L = 96b$ and $K_a = 4000$. (B) Persistence length of the polymer at $L = 96b$ as a function of K_a.

interaction energy U_a as a function of time for the polymers at $L = 50b$ and $96b$. At each chain length, two typical chain rigidities, that is, $K_a = 0$ for the very flexible polymer and $K_a = 4000$ for the very stiff polymer, are considered in this figure. As U_a depends on the conformation of the polymer chain at the nanotube interface, these plots indicate the conformational transition process of the polymers during the wrapping procedure.[17,18] It is obvious that the very flexible polymers at $K_a = 0$ reach their equilibrium values at the very initial stage, independent of the chain length. However, at $K_a = 4000$ the energy trajectories at these both chain lengths are quite different from each other and from those at $K_a = 0$. In this case, the energy trajectories at $L = 50b$ and $96b$ initially undergo a fluctuation process at a high level of U_a and then decrease gradually to their equilibrium values. First the result of Figure 2A clarifies again that the chain length dependent interaction only takes place in the stiff polymer because there is almost no difference in the energy trajectories of both the short and the long polymers at $K_a = 0$. Second, the presence of the initial fluctuation process at a high level of U_a reveals that the conformational transition of the stiff polymer needs to overcome an energy barrier, which will be discussed in the following section. Finally, the equilibrium U_a at $K_a = 4000$ for the long polymer is much larger than that for the short polymer, demonstrating that the polymer−nanotube attraction is considerably weakened for the long stiff polymer.

The free energy of a stiff polymer consists of two opposing contributions, that is, the elastic energy U_e driving toward a rigid conformation and the entropy energy $U_s = -TS$ (S denotes the entropy) favoring random chain configuration. At the large value of K_a, the elastic energy penalty due to bending the stiff polymer adsorbed on the SWNT surface is much larger than the decrease of the entropy energy due to the spatial restriction of the polymer on the nanotube surface.[30] Thereby, the free energy of the stiff polymer is dominated by the elastic energy U_e, which provides the energy barrier for the initial conformational transition of the stiff polymers as indicated by the plots in Figure 2A. U_e can be calculated with $U_e/k_BT = l_p l/2R_0^2$,[20] where l_p is the persistence length of the polymer chain and Figure 2B plots l_p as a function of K_a in the present simulations.[31] The l is the bent part of the wrapped polymer and R_0 is the radius of curvature of the centerline of the wrapped polymer. Considering a perfect helical conformation where the polymer wraps the nanotube exactly along its threadline, the elastic energy of the long polymer with $l = L = 96b$ is about $2.5k_BT$ per bead at $K_a = 4000$, much larger than the absolute value of the polymer−nanotube attraction energy U_a. Thus, although the energy of the solvent−polymer interaction can also prompt the compactness of the polymer on the nanotube surface, both of these energies cannot make the long stiff polymer holding a perfect helical conformation. Indeed, as shown in Figure 1B, the long stiff polymer does not bend uniformly when $K_a > 300$, which enlarges the local R_0 and reduces its elastic energy. Actually, even in the helical conformation of the short polymer at $L = 50b$, the polymer does not wrap exactly along the threadline of the nanotube in order to decrease its elastic energy.

Figure 3 shows three typical local conformations of the stiff polymer on the nanotube surface, that is, helical wrapping along

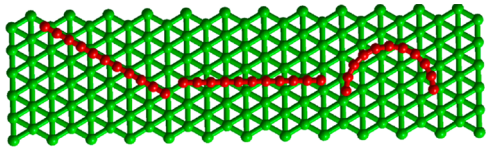

Figure 3. Schematic representation of three typical local conformations of the stiff polymer on the SWNT surface: (left) helical wrapping along the nanotube threadline, (middle) straight extension along the nanotube, and (c) nonhelical loop. Here the SWNT is unwrapped into a graphene sheet to display the detailed relations between the beads of the polymer and the nanotube.

the nanotube threadline, straight extension along the nanotube and nonhelical loop, where a short chain with 11 beads is used as a model of the polymer. To display the detailed relations between the beads of the polymer and the nanotube, the SWNT is unwrapped into a planar graphene sheet. The last two conformations are preferred by the long stiff polymer due to their lower elastic energies. We calculate the polymer−nanotube interaction U_a of these three conformation and find $U_a = -0.102\ k_BT$, $-0.0976k_BT$, and $-0.0993k_BT$ from left to right. Clearly, the helical wrapping along the nanotube threadline is the most stable conformation. However, in contrast to the short polymer, the large length of the long stiff polymer provides difficulty to its conformation adjustment toward this ideal conformation. In addition to the barrier from the high elastic energy of the stiff polymer, the match between the polymer beads and the structural details of the underlying nanotube surface is impaired as demonstrated by the last two conformations, weakening the polymer−nanotube attraction.

To gain more detailed insight into the effect of chain length, we determine U_a as a function of chain length at $K_a = 0$ and 5000, respectively (Figure 4). What is interesting is that, at $K_a = 5000$, U_a first decreases with the increases of L and then

dx.doi.org/10.1021/mz300221s | ACS Macro Lett. 2012, 1, 977−981

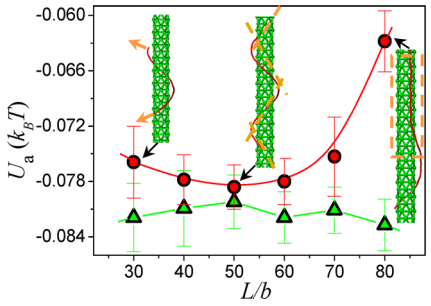

Figure 4. U_a as a function of the contour length of the polymer, L, at $K_a = 0$ (green) and $K_a = 5000$ (red). The solid lines are to guide the eye. The insets show the enlarged conformations of the stiff polymers at various chain lengths denoted by the black arrows.

increases from $L > 50b$, while at $K_a = 0$ it only presents a slight fluctuation within the chain lengths concerned. At about $L = 50b$, U_a reaches a minimum for the stiff polymer. The presence of the energy minimum reveals that the corresponding chain length is preferred in the structural formation of the polymer-nanotube complex because the polymer-nanotube attraction is strongest at this length. The preferred length of the stiff polymer can be rationalized by considering the detailed structures of the complexes shown in the insets of Figure 4. Recall that the persistence length of the stiff polymer at $K_a = 5000$ is about $l_p = 48b$ (Figure 2B), very close to the preferred length of the stiff polymer. Thus, when the chain length is shorter than the preferred length, the polymer deforms as a bendable rod. In this case, the stiff polymer is difficult to overcome the elastic energy to perfectly wrap the nanotube along its threadline. Moreover, the short polymer cannot fully wrap the nanotube, and their two ends tend to detach from the nanotube, as indicated by the arrows in the left inset of Figure 4. With the increase of chain length, the deformation of the stiff polymer becomes easier, which facilitates its conformation transition to match the threadline of the pitch angle of the nanotube. Thus, at about one persistence length, the stiff polymer reaches the perfect helical conformation as indicated by the dashed line in the middle inset of Figure 4. However, chains comprising many persistent segments tend to a random walk. In addition to the elastic energy barrier, increasing further chain length really adds the difficulty to the match between the polymer beads and the nanotube threadline. Then the local conformations of nonhelical loop and straight extension along the nanotube occur in the long stiff polymer as marked by the rectangle in the right inset of Figure 4. As stated above, these two local conformations turn to weaken the polymer−nanotube attraction.

By this token, our simulations reveal the presence of the preferred chain length with an energy minimum in the self-assemble of a stiff polymer on the carbon nanotube surface. Further, the simulated results predict that the preferred length occurs at about one persistence length of the stiff polymer, which also provides an effective approach to guide the relevant experimental design because the persistence length is an important physical parameter characterizing the stiffness of the polymer chain and having a direct relation with the specific chemical structure.[32] Experimentally, the persistence length of a polymer can be measured through various techniques, for example, the scattering measurements,[33,34] and can also be readily obtained from the literature.[32] For instance, the persistence length of polypropylene (PP) with a very flexible chain is about 0.55 nm[32] while the value of polyfluorene (PF) with stiff chain is about 8.0 nm.[33] In view of the simulation results, the self-assembly of the PF chain on the SWNT surface will exhibit a more obviously length-dependent effect and the preferred PF chain length in the assembly might occur at about 8.0 nm. Our hope is that these predictions can stimulate and facilitate corresponding experiments to further study the length-dependent effect in the self-assembly of a stiff polymer chain at the interface of a carbon nanotube.

In conclusion, our simulations demonstrate that the chain length plays a significant role in the conformation and interaction of the stiff polymer in its self-assembly at the nanotube interface, while this effect is considerably slight for the flexible polymer. It is revealed that the high elastic energy penalty and the large length of a long stiff polymer hinder its conformation transition on the nanotube, which impairs the match between the polymer beads and the nanotube threadline and thereby weakens the polymer−nanotube attraction. A preferred chain length with an energy minimum is documented for the first time in the self-assembly of a stiff polymer at the nanotube interface. For the implications of our results, two things are emphasized here. The first is that the chain length effect and the presence of the preferred chain length in the stiff polymer−nanotube interaction provide a new insight into the application of chain-like polymers in the purification, modification, and functionalization of carbon nanoparticles. The second is that the length effect of the stiff chain and the physical mechanism demonstrated in the letter can be applicable to the generic physical problem of a stiff string interacting with the detailed structures of a cylindrical surface. For example, in the nucleosome of chromatin, the DNA of rigid chain is coiled in almost two turns of a helix around a short cylinder of histone octamer.[20−22] This structure might be rationalized by the chain length effect because longer protein cylinder could incur nonhelical loop conformation in the DNA chain, weakening their interaction. In fact, the most stable complex in the present simulations also lies at the wrapping of the stiff polymer around the nanotube in almost two turns of a helix (see the middle inset of Figure 4).

AUTHOR INFORMATION

Corresponding Author

*E-mail: ltyan@mail.tsinghua.edu.cn.

Author Contributions

†These authors contributed equally.

Notes

The authors declare no competing financial interest.

ACKNOWLEDGMENTS

Financial support from the National Natural Science Foundation of China (No. 21174080) is greatly appreciated.

REFERENCES

(1) Hersam, M. C. *Nat. Nanotechnol.* **2008**, *3*, 387−394.
(2) Hirsh, J. *Angew. Chem., Int. Ed.* **2002**, *41*, 1853−1859.
(3) Nishi, A.; Hwang, J. -Y.; Doig, J.; Nicholas, R. J. *Nat. Nanotechnol.* **2007**, *2*, 640−646.
(4) Numata, M.; Asai, M.; Kaneko, K.; Bae, A. H.; Hasegawa, T.; Sakurai, K.; Shinkai, S. *J. Am. Chem. Soc.* **2005**, *127*, 5875−5884.
(5) Dieckmann, G. R.; Dalton, A. B.; Johnson, P. A.; Razal, J.; Chen, J.; Giordano, G. M.; Munoz, E.; Musselman, I. H.; Baughman, R. H.; Draper, R. K. *J. Am. Chem. Soc.* **2003**, *125*, 1770−1777.

(6) Zheng, M.; Jagota, A.; Semke, E. D.; Diner, B. A.; Mclean, R. S.; Lustig, S. R.; Richardson, R. E.; Tassi, N. G. *Nat. Mater.* **2003**, *2*, 338−342.
(7) Ulrich, S.; Laguecir, A.; Stoll, S. *Macromolecules* **2005**, *38*, 8939−8949.
(8) Chen, Y.; Xu, Y.; Perry, K.; Sokolov, A.; More, K.; Pang, Y. *ACS Macro Lett.* **2012**, *1*, 701−705.
(9) Ozawa, H.; Fujigaya, T.; Niidome, Y.; Hotta, N.; Fujiki, M.; Nakashima, N. *J. Am. Chem. Soc.* **2011**, *133*, 2651−2657.
(10) Ozawa, H.; Ide, N.; Fujigaya, T.; Niidome, Y.; Nakashima, N. *Chem. Lett.* **2011**, *40*, 239−241.
(11) Kang, Y. K.; Lee, O. S.; Deria, P.; Kim, S. H.; Park, T. H.; Bonnell, D. A.; Saven, J. G.; Therien, M. J. *Nano Lett.* **2009**, *9*, 1414−1418.
(12) Gurevitch, I.; Srebnik, S. *J. Chem. Phys.* **2008**, *128*, 144901.
(13) Yang, M.; Koutsos, V.; Zaiser, M. *J. Phys. Chem. B* **2005**, *109*, 10009.
(14) Milchev, A.; Binder, K. *J. Chem. Phys.* **2002**, *117*, 6852−6862.
(15) Pincus, P. A.; Sandroff, C. J.; Witten, T. A. *J. Phys.* **1984**, *45*, 725−729.
(16) Naito, M.; Nobusawa, K.; Onouchi, H.; Nakamura, M.; Yasui, K.; Ikeda, A.; Fujiki, M. *J. Am. Chem. Soc.* **2008**, *130*, 16697−16703.
(17) Wei, C. *Nano Lett.* **2006**, *6*, 1627−1631.
(18) Wallace, E. J.; Sansom, M. S. P. *Nano Lett.* **2007**, *7*, 1923−1928.
(19) Saric, A.; Pamies, J. C.; Cacciuto, A. *Phys. Rev. Lett.* **2010**, *104*, 226101.
(20) Schiessel, H. *J. Phys.: Condens. Matter* **2003**, *15*, R699.
(21) Kulic, I. M.; Schiessel, H. *Phys. Rev. Lett.* **2003**, *91*, 148103.
(22) Kulic, I. M.; Schiessel, H. *Phys. Rev. Lett.* **2004**, *92*, 228101.
(23) Liba, O.; Kauzlaric, D.; Abrams, Z. R.; Hanein, Y.; Greiner, A.; Korvink, J. G. A. *Mol. Simul.* **2008**, *34*, 737−748.
(24) Yan, L. −T.; Guo, R. *Soft Matter* **2012**, *8*, 660−666.
(25) Groot, R. D.; Warren, P. B. *J. Chem. Phys.* **1997**, *107*, 4423−4435.
(26) Alexeev, A.; Uspal, W. E.; Balazs, A. C. *ACS Nano* **2008**, *2*, 1117−1122.
(27) Allen, M. P.; Tildesley, D. J. *Computer Simulation of Liquids*; Clarendon Press: Oxford, 1987.
(28) Peter, C.; Kremer, K. *Soft Matter* **2009**, *5*, 4357−4366.
(29) Vattulainen, I.; Karttunen, M.; Besold, G.; Polson, J. M. *J. Chem. Phys.* **2002**, *116*, 3967−3979.
(30) Kusner, I.; Srebnik, S. *Chem. Phys. Lett.* **2006**, *430*, 84−88.
(31) Micka, U.; Kremer, K. *J. Phys.: Condens. Matter* **1996**, *8*, 9463−70.
(32) Rubinstein, M.; Colby, R. H. *Polymer Physics*; Oxford University Press: New York, 2003.
(33) Fytas, G.; Nothofer, H. G.; Scherf, U.; Vlassopoulos, D.; Meier, G. *Macromolecules* **2002**, *35*, 481−488.
(34) Muller, F.; Manet, S.; Jean, B.; Chambat, G.; Boue, F.; Heux, L.; Cousin, F. *Biomacromolecules* **2011**, *12*, 3330−3336.